

An adaptive finite element method for the inequality-constrained Reynolds equation

Tom Gustafsson^a, Kumbakonam R. Rajagopal^b, Rolf Stenberg^a,
Juha Videman^c

^a*Aalto University, Department of Mathematics and Systems Analysis, P.O. Box 11100
FI-00076 Aalto, Finland*

^b*Department of Mechanical Engineering, Texas A&M University, 3123 College Station, TX
77843-3123, USA*

^c*CAMGSD and Mathematics Department, Instituto Superior Técnico, Universidade de
Lisboa, Av. Rovisco Pais 1, 1049-001 Lisboa, Portugal*

Abstract

We present a stabilized finite element method for the numerical solution of cavitation in lubrication, modeled as an inequality-constrained Reynolds equation. The cavitation model is written as a variable coefficient saddle-point problem and approximated by a residual-based stabilized method. Based on our recent results on the classical obstacle problem, we present optimal a priori estimates and derive novel a posteriori error estimators.

The method is implemented as a Nitsche-type finite element technique and shown in numerical computations to be superior to the usually applied penalty methods.

1. Introduction

Friction is an ever present phenomenon between solid surfaces that are in contact and move with respect to each other. In order to reduce the wear and tear of such sliding surfaces one uses a lubricant.

The lubricant film thickness is often small in comparison to the characteristic dimensions of the lubricated object. Assuming that the flow in such thin films can be modeled by the Navier–Stokes fluid, Reynolds obtained an approximation to the equations of motion [1]. This approximation, known as the Reynolds equation, has proved to be invaluable, however the equations have unfortunately also been misused and misapplied to various problems wherein the basic assumptions that Reynolds made are not met. In some cases, generalizations have been made that are incorrect (see the discussion in Rajagopal and Szeri [2]).

Although liquids can sustain negative pressures to some extent, it is of particular interest to model the cavitation phenomenon which is known to occur in tribological environments under strong sub-atmospheric pressures, cf. Braun–Hannon [3] for a fairly recent review on the subject from a modeling perspective.

The described physical conditions result in a rupture of the lubricant film causing the formation of cavities that are filled by a mixture of gas and vapor, cf. the experimental results and pictures, e.g., in Xing et al. [4].

A direct application of the Reynolds equation in the full 360° journal bearing geometry leads to a pressure field with equal positive and negative pressure spikes in the converging and diverging regions, respectively. As this obviously cannot hold true for large negative pressures due to cavitation, different attempts have been made to incorporate cavitation into the Reynolds equation.

The most rudimentary approach for taking into account the resulting film rupture—often accredited to Gumbel [5]—is to simply compute the pressure field p from the standard Reynolds equation and truncate it wherever it goes below a predetermined constant cavitation pressure value. Another possibility, put forward by Swift [6] and Stieber [7], is to impose the following cavitation zone formation conditions at the cavitation boundary:

$$\frac{\partial p}{\partial x} = \frac{\partial p}{\partial y} = 0, \quad p = p_c. \quad (1)$$

From a mathematical perspective these conditions transform the model into a free boundary problem that can be formulated as a variational inequality [8].

The Swift–Stieber or the variational inequality model has been criticized for not properly modeling the starvation phenomena where the cavitation region extends to the converging side of the flow region, cf. Bayada–Vázquez [9]. This has led to the development of alternative Reynolds-type cavitation models, see, e.g., Elrod–Adams [10], Vijayaraghavan–Keith [11], Bayada et al. [12, 13, 14, 15], Almqvist et al. [16], Garcia et al. [17], Mistry et al. [18], for different models and their applications. It has also been recently shown, within the context of fluids with pressure dependent viscosity, by Lanzendörfer et al. [19] that a solution based on using a cut-off value for the pressure to determine the region of cavitation is sensitive to the value of the cut-off. Nevertheless, it is obvious that any cavitation model derived from continuum mechanics involves an initially unknown region of cavitation and therefore it is mandatory to consider numerical methods that automatically capture the location of the cavitation region and adapt to the resulting free boundaries.

As a step towards better numerical modeling of cavitation, we study the numerical solution of the Reynolds model with Swift–Stieber cavitation conditions using adaptive finite element techniques. Similarly to our recent work on the obstacle problem [20], the positivity constraint of the pressure field is imposed using the Lagrange multiplier technique instead of the more traditional penalty method since adaptive penalty methods easily lead to over-refinement in the cavitation area [21, 22]. The resulting variational inequality has a saddle-point structure and must be solved either by using a carefully designed pair of mixed finite element spaces or by a stabilized method in the spirit of Hughes–Franca [23]. In this work, we choose the latter approach since the discontinuous Lagrange multiplier can be eliminated elementwise from the discrete linearized problem, cf. Section 5. The resulting formulation involves only positive definite linear systems that are fast to assemble [20].

Cavitation is a very daunting problem which is yet to be thoroughly addressed. In fact, if one were to carry out a meaningful study of the problem, one should adopt a fully thermodynamic approach as there can be dissipation in the viscous lubricant leading to an increase of the lubricant temperature. In certain applications, this increase can be significant thereby leading to a change in the viscosity. Complicating matters further is the fact that the cavity is not necessarily a vacuum but contains the vapor of the lubricant and possibly trapped air, in other words a material for which one needs a thermodynamic equation of state. Temperature can have a major role in the initiation of cavitation and also in determining the vapor pressure within the cavity. Moreover, one may need to take into account the surface tension at the boundary of the cavity and solve the interaction problem between the fluid and the cavity that is constantly changing with space and time. Furthermore, the state of the fluid prior to the initiation of cavitation can be such that one might have to take compressibility effects into consideration. Of course, one cannot account for all these issues simultaneously as the problem would become intractable. A sensible approach is to consider first the simplest approximation that yet captures the quintessential features of the problem, and then add more of the physically relevant issues. This is precisely the approach that we adopt in this work.

For previous studies of adaptive finite element techniques applied to cavitation modeling, we refer to Wu–Oden [24], Nilsson–Hansbo [25] and Sorsimo et al. [22]. In all these works, the classical penalty method was used to enforce the constraint $p \geq p_c$. The error estimator in the early study of Wu–Oden [24] was based on the simplistic idea of minimizing the large gradients present in the solution. The more recent works of Nilsson–Hansbo [25] and Sorsimo et al. [22] were built upon the a posteriori estimates derived by Johnson [26] for the obstacle problem in the penalty formulation.

Some shortcomings of the penalty method approach, when applied to the obstacle problem of an elastic membrane, are discussed in [27]. They include:

- Nonconformity of the method. This means that the convergence rate is optimal for linear elements only.
- Condition numbers of the resulting linear systems increase faster than for standard finite elements of the same polynomial order.
- The method can lead to over-refinement if the penalty parameter is not chosen appropriately.

As shown in our earlier works [20, 27], none of these issues arise from the stabilized finite element formulation of variational inequalities. Thus, the main goal of this work is to investigate the suitability of stabilized finite element methods for the approximation of the Reynolds’ cavitation model and, at the same time, establish novel a posteriori error estimators for variable coefficient elliptic variational inequalities. To our knowledge, this is the first time when suitably modified residual based a posteriori error estimators and stabilizing terms have been presented for variable coefficient saddle-point problems, see [28, 29] for similar a posteriori error analyses of elliptic equations.

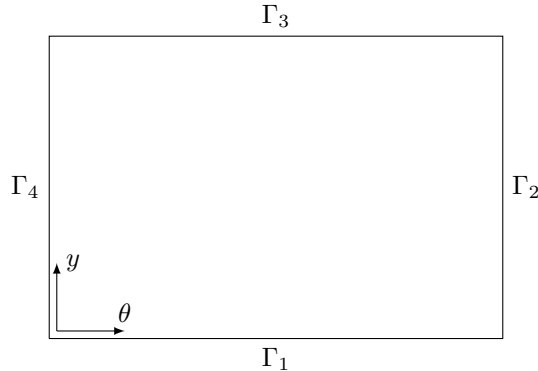


Figure 1: Let p denote the pressure field. Typical boundary conditions for the pressure field in the full periodic 360° journal bearing geometry are $p|_{\Gamma_1} = p|_{\Gamma_3} = 0$ (constant atmospheric pressure) and $p(\theta, y) = p(\theta + 2\pi, y)$, $\theta \in \Gamma_4$ (periodic boundary condition). Moreover, for the periodic boundaries we have $\frac{\partial p}{\partial \theta}(\theta, y) = \frac{\partial p}{\partial \theta}(\theta + 2\pi, y)$, $\theta \in \Gamma_4$. Sometimes (for example in locomotive applications) the journal is in contact with the bearing surface only on a part of the journal boundary. Then the width of the domain is less than 2π and the boundary conditions are simply $p|_{\Gamma_i} = 0$, $i \in \{1, 2, 3, 4\}$.

2. Reynolds equation

Derivation of the Reynolds equation from the Navier–Stokes equations is standard and can be found, e.g., in [30, 31]. The assumptions are the following:

- The lubricant is homogeneous, incompressible and Newtonian, i.e. the Navier–Stokes equations are valid.
- The flow takes place between two almost parallel surfaces with the distance between the surfaces given by a function $d : \mathbb{R}^2 \rightarrow \{x \in \mathbb{R} : x > 0\}$.
- The fluid film thickness d is small with respect to the characteristic lengths along other directions.
- The curvature of the surfaces is negligible.
- The flow is slow enough or the viscosity μ high enough so that the lubricant inertia can be ignored.

In this work, we consider steady-state flow regime and assume that the viscosity μ remains constant. Note, however, that our results are valid also for the equation arising from a fixed-point linearization of the Reynolds equation with a moderate pressure-dependency of μ as shown in [32]. Compressibility, curvature and inertia effects can be taken into account by a suitable modification of the Reynolds equation, for the latter two we refer to [33].

Let $\Omega \subset \mathbb{R}^2$ be the computational domain representing both the lubricated and the cavitated region. Assume that the relative velocity between the surfaces

has magnitude U and the direction is (locally) parallel to the x -axis. The Reynolds equation for the unknown pressure field $p : \Omega \rightarrow \mathbb{R}$ reads as

$$-\operatorname{div} \left(\frac{d^3}{\mu} \nabla p \right) = -6U \frac{\partial d}{\partial x}. \quad (2)$$

Equation (2) is complemented with appropriate boundary conditions for p .

Remark 1. In the journal bearing geometry, we have $x = R\theta$, $U = R\omega$ and $d(\theta) = c_1(1 + \varepsilon \cos(\theta - \varphi))$ where R is the radius of the bearing, ω is the angular velocity and (c_1, ε) are geometrical parameters; $\varepsilon \in (0, 1)$ is the eccentricity of the bearing, c_1 is the minimum film thickness and φ determines the location of the minimum film thickness (due to external loading on the journal). The Reynolds equation becomes

$$-\frac{\partial}{\partial \theta} \left(d^3 \frac{\partial p}{\partial \theta} \right) - R^2 \frac{\partial}{\partial y} \left(d^3 \frac{\partial p}{\partial y} \right) = -6\mu\omega R^2 \frac{\partial d}{\partial \theta} \quad \text{in } \Omega, \quad (3)$$

where

$$\Omega = \{(\theta, y) : 0 \leq \theta \leq \psi, \quad 0 \leq y \leq L\}.$$

Here, L is the width of the finite bearing and $0 < \psi \leq 2\pi$ defines the extent of the bearing surface. The boundary conditions are shown in Figure 1 and are different for $\psi = 2\pi$ and $\psi < 2\pi$.

Remark 2. The Reynolds equation (3) can be normalized defining the non-dimensionalized variables

$$\bar{d} = \frac{d}{c_1}, \quad \bar{y} = \frac{y}{L}, \quad \bar{p} = \frac{p}{\mu\omega} \left(\frac{c_1}{R} \right)^2. \quad (4)$$

This leads to

$$-\frac{\partial}{\partial \theta} \left(\bar{d}^3 \frac{\partial \bar{p}}{\partial \theta} \right) - \left(\frac{R}{L} \right)^2 \frac{\partial}{\partial \bar{y}} \left(\bar{d}^3 \frac{\partial \bar{p}}{\partial \bar{y}} \right) = -6 \frac{\partial \bar{d}}{\partial \theta}. \quad (5)$$

The Swift–Stieber cavitation model corresponds to imposing the constraint $p \geq p_c$ where p_c is the cavitation pressure. The momentum balance (2) holds true only in the lubricated region where p is strictly greater than p_c . In the cavitation region $p = p_c$. Hence, the governing equations read as

$$-\mathcal{A}(p) \geq f, \quad \text{in } \Omega, \quad (6)$$

$$p - p_c \geq 0, \quad \text{in } \Omega, \quad (7)$$

$$(\mathcal{A}(p) + f)(p - p_c) = 0, \quad \text{in } \Omega, \quad (8)$$

$$(9)$$

where we have set $f = -6\mu U \frac{\partial d}{\partial x}$ and defined

$$\mathcal{A}(p) = \operatorname{div} (d^3 \nabla p). \quad (10)$$

The boundary conditions are

$$p|_{\Gamma_1 \cup \Gamma_3} = 0, \quad (11)$$

$$p|_{\Gamma_2} = p|_{\Gamma_4}, \quad (12)$$

$$(\nabla p \cdot \mathbf{n})|_{\Gamma_2} = (\nabla p \cdot \mathbf{n})|_{\Gamma_4}, \quad (13)$$

for the full 360° journal bearing and

$$p|_{\partial\Omega} = 0, \quad (14)$$

for smaller contact angles, see the explanations in the caption of Figure 1. Note that the cavitation zone formation conditions (1) are implicitly satisfied inside and on the boundary of the cavitation region.

In the following chapters we formulate the variational inequality using the simpler boundary condition (14) although everything holds true also in the case of a periodic boundary condition.

3. Variational inequality and its discretization

Aiming at solving the problem (6)–(13) by the finite element method, we first write it in a variational form. A method best suited to adaptive solution strategies includes an additional unknown $\lambda : \Omega \rightarrow \{x \in \mathbb{R} : x \geq 0\}$, a Lagrange multiplier function positive in the cavitation region and zero elsewhere. The equations (6)–(8) are then transformed to

$$-\mathcal{A}(p) - \lambda = f, \quad (15)$$

$$p - p_c \geq 0, \quad (16)$$

$$(p - p_c)\lambda = 0. \quad (17)$$

Let us introduce the variational spaces

$$Q = \{q \in H^1(\Omega) : q|_{\partial\Omega} = 0\}, \quad (18)$$

$$\Lambda = \{\mu \in H^{-1}(\Omega) : \langle q, \mu \rangle \geq 0 \ \forall q \in Q, \ q \geq 0 \text{ a.e. in } \Omega\}, \quad (19)$$

equipped with the energy norm $\|\cdot\|$ and its dual norm $\|\cdot\|_*$ defined by

$$\|r\|^2 = \int_{\Omega} d^3(\nabla r)^2 \, d\mathbf{x} \quad \text{and} \quad \|\xi\|_* = \sup_{q \in Q} \frac{\langle q, \xi \rangle}{\|q\|}, \quad (20)$$

where $\langle \cdot, \cdot \rangle : Q \times H^{-1}(\Omega) \rightarrow \mathbb{R}$ denotes the duality pairing. Defining the bilinear and linear forms through

$$\mathcal{B}(r, \xi; q, \mu) = \int_{\Omega} d^3 \nabla r \cdot \nabla q \, d\mathbf{x} - \langle q, \xi \rangle - \langle r, \mu \rangle,$$

$$\mathcal{L}(q, \mu) = \int_{\Omega} f q \, d\mathbf{x} - \langle p_c, \mu \rangle,$$

we arrive at the following variational inequality formulation of problem (15)–(17), (11)–(13).

Problem 1 (Continuous variational problem). *Find $(p, \lambda) \in Q \times \Lambda$ satisfying*

$$\mathcal{B}(p, \lambda; q, \mu - \lambda) \leq \mathcal{L}(q, \mu - \lambda) \quad (21)$$

for every $(q, \mu) \in Q \times \Lambda$.

Remark 3. Formulation (21) can also be derived by applying the method of Lagrange multipliers to the constrained energy minimization problem

$$\inf_{q \in Q, q \geq p_c} \frac{1}{2} \|q\|^2 - \int_{\Omega} f q \, d\mathbf{x}. \quad (22)$$

The following stability estimate guarantees the well-posedness of Problem 1. The stability result of Theorem 1 is also crucial for the a posteriori error analysis presented in the next section.

Theorem 1 (Continuous stability). *For all $(r, \xi) \in Q \times H^{-1}(\Omega)$ there exists $q \in Q$ such that with some constants $C_1, C_2 > 0$ it holds*

$$\mathcal{B}(r, \xi; q, -\xi) \geq C_1 (\|r\| + \|\xi\|_*)^2 \quad \text{and} \quad \|q\| \leq C_2 (\|r\| + \|\xi\|_*). \quad (23)$$

Proof. Choose $q = r - r_{\xi}$ where $r_{\xi} \in Q$. Then by linearity and Cauchy–Schwarz inequality

$$\mathcal{B}(r, \xi; r - r_{\xi}, -\xi) \geq \|r\|^2 - \|r\| \|r_{\xi}\| + \langle r_{\xi}, \xi \rangle. \quad (24)$$

We now fix $r_{\xi} \in Q$ as the solution of the auxiliary problem

$$\int_{\Omega} d^3 \nabla r_{\xi} \cdot \nabla q \, d\mathbf{x} = \langle q, \xi \rangle, \quad \forall q \in Q. \quad (25)$$

For such r_{ξ} , a standard reasoning shows that $\langle r_{\xi}, \xi \rangle = \|r_{\xi}\| = \|\xi\|_*$, cf. [20]. The upper bound for $\|r\| + \|\xi\|_*$ now follows from Young’s inequality. The lower bound is a direct consequence of the triangle inequality. \square

We will approximate the (saddle-point) Problem 1 by a stabilized finite element method, instead of a mixed method, to avoid the Babuška-Brezzi inf-sup condition. Let \mathcal{C}_h denote the discretization of Ω into triangular elements $K \in \mathcal{C}_h$ with h_K referring to the local mesh parameter and $h = \max_{K \in \mathcal{C}_h} h_K$. The discrete finite element spaces $Q_h \subset Q$ and $\Lambda_h \subset L^2(\Omega)$ are defined as

$$Q_h = \{q_h \in Q : q_h|_K \in P_k(K) \, \forall K \in \mathcal{C}_h\}, \quad (26)$$

$$\Lambda_h = \{\mu_h \in L^2(\Omega) : \mu_h|_K \in P_l(K) \, \forall K \in \mathcal{C}_h\}, \quad (27)$$

where $k \geq 1$ and $l \geq 0$ are the polynomial degrees. We further denote by Λ_h^+ the following subset of Λ_h

$$\Lambda_h^+ = \{\mu_h \in \Lambda_h : \mu_h \geq 0 \text{ a.e. in } \Omega\}. \quad (28)$$

Let $\alpha > 0$ be a stabilization parameter. We introduce the following discrete bilinear and linear forms

$$\begin{aligned}\mathcal{B}_h(r, \xi; q, \mu) &= \mathcal{B}(r, \xi; q, \mu) - \alpha \sum_{K \in \mathcal{C}_h} \frac{h_K^2}{d_K^3} \int_K (-\mathcal{A}(r) - \xi)(-\mathcal{A}(q) - \mu) \, d\mathbf{x}, \\ \mathcal{L}_h(q, \mu) &= \mathcal{L}(q, \mu) - \alpha \sum_{K \in \mathcal{C}_h} \frac{h_K^2}{d_K^3} \int_K f(-\mathcal{A}(q) - \mu) \, d\mathbf{x},\end{aligned}$$

where d_K represents the mean value of d inside the element K . Note that, in contrast to the obstacle problem with a constant material parameter, here a proper scaling by d_K is mandatory as the film thickness function d^3 may vary several orders of magnitude inside the domain in practical lubrication problems.

Problem 2 (Stabilized finite element method). *Find $(p_h, \lambda_h) \in Q_h \times \Lambda_h^+$ satisfying*

$$\mathcal{B}_h(p_h, \lambda_h; q_h, \mu_h - \lambda_h) \leq \mathcal{L}_h(q_h, \mu_h - \lambda_h) \quad (29)$$

for every $(q_h, \mu_h) \in Q_h \times \Lambda_h^+$.

To simplify the estimates, we will assume that $d \in C^1(\Omega)$ and that for a given mesh \mathcal{C}_h there exists global positive constants γ_1 and γ_2 so that

$$\gamma_1 \min_{\mathbf{x} \in K} d(\mathbf{x}) \leq d(\mathbf{y}) \leq \gamma_2 \max_{\mathbf{x} \in K} d(\mathbf{x}) \quad (30)$$

for any element $K \in \mathcal{C}_h$ and at every point $\mathbf{y} \in K$. Generalization to a non-smooth d would be straightforward following the reasoning presented in [28], see also [34].

Theorem 2 (Discrete stability). *Suppose that $0 < \alpha < C_I$ where C_I is the constant of the inverse inequality*

$$C_I \sum_{K \in \mathcal{C}_h} \frac{h_K^2}{d_K^3} \|\mathcal{A}(q_h)\|_{0,K}^2 \leq \|q_h\|^2 \quad \forall q_h \in Q_h. \quad (31)$$

Then for all $(r_h, \xi_h) \in Q_h \times \Lambda_h$ there exists $q_h \in Q_h$ such that for some $C_1, C_2 > 0$ it holds

$$\mathcal{B}_h(r_h, \xi_h; q_h, -\xi_h) \geq C_1 (\|r_h\| + \|\xi_h\|_*)^2, \quad (32)$$

and

$$\|q_h\| \leq C_2 (\|r_h\| + \|\xi_h\|_*). \quad (33)$$

Proof. Using the inverse inequality (31), we get

$$\begin{aligned}\mathcal{B}_h(r_h, \xi_h; r_h, -\xi_h) &= \|r_h\|^2 - \alpha \sum_{K \in \mathcal{C}_h} \frac{h_K^2}{d_K^3} \|\mathcal{A}(r_h)\|_{0,K}^2 + \alpha \sum_{K \in \mathcal{C}_h} \frac{h_K^2}{d_K^3} \|\xi_h\|_{0,K}^2 \\ &\geq \left(1 - \frac{\alpha}{C_I}\right) \|r_h\|^2 + \alpha \sum_{K \in \mathcal{C}_h} \frac{h_K^2}{d_K^3} \|\xi_h\|_{0,K}^2.\end{aligned}$$

Following the general steps presented in [20, Theorem 4.1], we can construct $\tilde{q}_h \in Q_h$ which satisfies

$$\mathcal{B}_h(r_h, \xi_h; \tilde{q}_h, 0) \geq C_3 \|\xi_h\|_*^2 - C_4 \left(\|r_h\|^2 + \sum_{K \in \mathcal{C}_h} \frac{h_K^2}{d_K^3} \|\xi_h\|_{0,K}^2 \right)$$

with some positive constants C_3 and C_4 . Hence by bilinearity

$$\begin{aligned} \mathcal{B}_h(r_h, \xi_h; r_h + \delta \tilde{q}_h, -\xi_h) &= \mathcal{B}_h(r_h, \xi_h; r_h, -\xi_h) + \delta \mathcal{B}_h(r_h, \xi_h; \tilde{q}_h, 0) \\ &\geq \left(1 - \frac{\alpha}{C_I} - \delta C_4 \right) \|r_h\|^2 + \delta C_3 \|\xi_h\|_*^2 \\ &\quad + (\alpha - \delta C_4) \sum_{K \in \mathcal{C}_h} \frac{h_K^2}{d_K^3} \|\xi_h\|_{0,K}^2, \end{aligned}$$

where for any given $\alpha \in (0, C_I)$ the positive parameter δ can be chosen in such a way that all terms on the right hand side remain positive. \square

Theorem 3. *Let $f_h \in Q_h$ be the L^2 -projection of f and suppose that $0 < \alpha < C_I$. There exists $C > 0$ such that the following a priori estimate holds*

$$\begin{aligned} &\|p - p_h\| + \|\lambda - \lambda_h\|_* \tag{34} \\ &\leq C \left(\inf_{q_h \in Q_h} \|p - q_h\| + \inf_{\mu_h \in \Lambda_h^+} \left(\|\lambda - \mu_h\|_* + \sqrt{\int_{\Omega} (p - p_c) \mu_h \, d\mathbf{x}} \right) \right. \\ &\quad \left. + \sqrt{\sum_{K \in \mathcal{C}_h} \frac{h_K^2}{d_K^3} \|f - f_h\|_{0,K}^2} \right). \end{aligned}$$

This is essentially a best approximation result analogous to the well known Céa's lemma which holds for coercive variational problems. The proof is based on the stability result of Theorem 2 and can be found in [20]. The first two terms on the right hand side can be bounded from above using interpolation estimates. The third term is zero if the finite element mesh follows exactly the boundary of the cavitation region. In general this cannot be guaranteed a priori and adaptive methods are required to properly resolve the cavitation boundary.

4. Adaptive refinement

Let d_E stand for d 's mean value along the edge E . The following a posteriori error bounds demonstrate the suitability of our stabilized finite element method to adaptive solution strategies.

Theorem 4. *The following a posteriori estimate holds*

$$\begin{aligned}
& \| \|p - p_h\| \| + \| \lambda - \lambda_h \|_* \tag{35} \\
& \leq C \left(\sqrt{\sum_{K \in \mathcal{C}_h} \frac{h_K^2}{d_K^3} \| \mathcal{A}(p_h) + \lambda_h + f \|_{0,K}^2} + \sqrt{\sum_{E \in \mathcal{E}_h} \frac{h_E}{d_E^3} \| d^3 [\nabla p_h \cdot \mathbf{n}] \|_{0,E}^2} \right. \\
& \quad \left. + \| (p_c - p_h)_+ \| + \sqrt{\int_{\Omega} (p_h - g)_+ \lambda_h \, d\mathbf{x}} \right),
\end{aligned}$$

where the constant $C > 0$ is independent of h and d .

Proof. Since the proof goes as in [20], we will only outline the main steps and refer to [20] for further details.

In view of Theorem 1, there exists $q \in Q$ such that

$$\| \|q\| \| \leq C_2 (\| \|p - p_h\| \| + \| \lambda - \lambda_h \|_*)$$

and

$$\begin{aligned}
& (\| \|p - p_h\| \| + \| \lambda - \lambda_h \|_*)^2 \\
& \leq C_1 \mathcal{B}(p - p_h, \lambda - \lambda_h; q, \lambda_h - \lambda) \\
& \leq C_1 (\mathcal{B}(p, \lambda; q, \lambda_h - \lambda) - \mathcal{B}(p_h, \lambda_h; q, \lambda_h - \lambda) - \mathcal{B}_h(p_h, \lambda_h; -\tilde{q}, 0) + \mathcal{L}_h(-\tilde{q}, 0)) \\
& \leq C_1 (\mathcal{L}(q - \tilde{q}, \lambda_h - \lambda) - \mathcal{B}(p_h, \lambda_h; q - \tilde{q}, \lambda_h - \lambda) \\
& \quad - \alpha \sum_{K \in \mathcal{C}_h} \frac{h_K^2}{d_K^3} (\mathcal{A}(p_h) + \lambda_h + f, \mathcal{A}(\tilde{q}))_{0,K}) \\
& = C_1 \left(\sum_{K \in \mathcal{C}_h} (\mathcal{A}(p_h) + \lambda_h + f, q - \tilde{q})_{0,K} - \sum_{E \in \mathcal{E}_h} (d^3 [\nabla p_h \cdot \mathbf{n}], q - \tilde{q})_{0,E} \right. \\
& \quad \left. + \langle p_h - p_c, \lambda_h - \lambda \rangle - \alpha \sum_{K \in \mathcal{C}_h} \frac{h_K^2}{d_K^3} (\mathcal{A}(p_h) + \lambda_h + f, \mathcal{A}(\tilde{q}))_{0,K} \right),
\end{aligned}$$

where $\tilde{q} \in Q_h$ is the Clément interpolant of q . Note that

$$0 \leq -\mathcal{B}_h(p_h, \lambda_h; -\tilde{q}, 0) + \mathcal{L}_h(-\tilde{q}, 0)$$

and that for some positive constants C' and C'' it holds

$$\left(\sum_{K \in \mathcal{C}_h} h_K^{-2} d_K^3 \| q - \tilde{q} \|_{0,K}^2 \right)^{1/2} + \left(\sum_{E \in \mathcal{E}_h} h_E^{-1} d_E^3 \| q - \tilde{q} \|_{0,E}^2 \right)^{1/2} \leq C' \| \|q\| \|,$$

and

$$\| \tilde{q} \| \| \leq C'' \| \|q\| \|.$$

Given that

$$\begin{aligned}
& \sum_{K \in \mathcal{C}_h} (\mathcal{A}(p_h) + \lambda_h + f, q - \tilde{q})_{0,K} \\
& \leq \sum_{K \in \mathcal{C}_h} \frac{h_K}{d_K^{3/2}} \|\mathcal{A}(p_h) + \lambda_h + f\|_{0,K} \frac{d_K^{3/2}}{h_K} \|q - \tilde{q}\|_{0,K}, \\
& \sum_{E \in \mathcal{E}_h} (d^3 \llbracket \nabla p_h \cdot \mathbf{n} \rrbracket, q - \tilde{q})_{0,E} \\
& \leq \sum_{E \in \mathcal{E}_h} \frac{h_E^{1/2}}{d_E^{3/2}} \|d^3 \llbracket \nabla p_h \cdot \mathbf{n} \rrbracket\|_{0,E} \frac{d_E^{3/2}}{h_E^{1/2}} \|q - \tilde{q}\|_{0,E}, \\
& \sum_{K \in \mathcal{C}_h} \frac{h_K^2}{d_K^3} (\mathcal{A}(p_h) + \lambda_h + f, \mathcal{A}(\tilde{q}))_{0,K} \\
& \leq \sum_{K \in \mathcal{C}_h} \frac{h_K}{d_K^{3/2}} \|\mathcal{A}(p_h) + \lambda_h + f\|_{0,K} \frac{h_K}{d_K^{3/2}} \|\mathcal{A}(\tilde{q})\|_{0,K},
\end{aligned}$$

and (cf. [20])

$$\langle p_h - p_c, \lambda_h - \lambda \rangle \leq \| (p_c - p_h)_+ \| \| \lambda - \lambda_h \|_* + \langle (p_h - p_c)_+, \lambda_h \rangle$$

one readily derives the upper bound for $\|p - p_h\| + \| \lambda - \lambda_h \|_*$ by combining the above estimates and using the inverse inequality (31). \square

In the next theorem we show the existence of a lower bound.

Theorem 5. *There exists a constant $C_1 > 0$ such that*

$$\begin{aligned}
& \left(\sum_{K \in \mathcal{C}_h} \frac{h_K^2}{d_K^3} \|\mathcal{A}(p_h) + \lambda_h + f\|_{0,K}^2 \right)^{1/2} + \left(\sum_{E \in \mathcal{E}_h} \frac{h_E}{d_E^3} \|d^3 \llbracket \nabla p_h \cdot \mathbf{n} \rrbracket\|_{0,E}^2 \right)^{1/2} \\
& \leq C_1 \left(\|p - p_h\| + \| \lambda - \lambda_h \|_* + \sqrt{\sum_{K \in \mathcal{C}_h} \frac{h_K^2}{d_K^3} \|f - f_h\|_{0,K}^2} \right).
\end{aligned}$$

Proof. Similarly to [20], we first derive local lower bounds. We start by defining, for any $q_h \in Q_h$ and $\mu_h \in \Lambda_h$ and in each K , a function γ_K by

$$\gamma_K = \frac{h_K^2}{d_K^3} b_K (\mathcal{A}(p_h) + \lambda_h + f_h)$$

where $b_K \in P_3(K) \cap H_0^1(K)$ is the usual bubble function, and let $\gamma_K = 0$ in $\Omega \setminus K$. Norm equivalence, equality (15) and integration by parts, imply that

$$\begin{aligned}
& \frac{h_K^2}{d_K^3} \|\mathcal{A}(q_h) + \mu_h + f_h\|_{0,K}^2 \\
& \leq C \frac{h_K^2}{d_K^3} \|\sqrt{b_K} (\mathcal{A}(q_h) + \mu_h + f_h)\|_{0,K}^2 = C (\mathcal{A}(q_h) + \mu_h + f_h, \gamma_K)_K \\
& \leq C ((d^3 \nabla(p - q_h), \nabla \gamma_K)_K + \langle \gamma_K, \mu_h - \lambda \rangle + (f_h - f, \gamma_K)_K) \\
& \leq C (\|p - q_h\|_K \| \gamma_K \|_K + \| \lambda - \mu_h \|_{*,K} \| \gamma_K \|_K + \|f - f_h\|_{0,K} \| \gamma_K \|_{0,K}),
\end{aligned}$$

where we have defined, for any $\mu \in \Lambda$,

$$\|\mu\|_{*,K} = \sup_{q \in H_0^1(K)} \frac{\langle q, \mu \rangle}{\|q\|_K}.$$

Here $q \in H_0^1(K)$ has been extended by zero into $\Omega \setminus K$. Using inverse estimates and norm equivalence, one easily shows that

$$\|\gamma_K\|_K^2 \leq C d_K^3 h_K^{-2} \|\gamma_K\|_{0,K}^2 \leq C \frac{h_K^2}{d_K^3} \|\mathcal{A}(q_h) + \mu_h + f_h\|_{0,K}^2.$$

Therefore,

$$\|f - f_h\|_{0,K} \|\gamma_K\|_{0,K} \leq C \left(\frac{h_K}{d_K^{3/2}} \|f - f_h\|_{0,K} \right) \left(\frac{h_K}{d_K^{3/2}} \|\mathcal{A}(q_h) + \mu_h + f_h\|_{0,K} \right).$$

Summing the above estimates over $K \in \mathcal{C}_h$ and choosing $q_h = p_h$ and $\mu_h = \lambda_h$ leads to the global lower bound in terms of the element residuals. We omit the proof of the bound in terms of the edge residuals since it is very similar, albeit a bit more technical, and has been proved in detail for a constant coefficient elliptic variational inequality in [20]. \square

Aiming at generating sequences of adaptively refined meshes, we define, in view of Theorem 4, an elementwise error estimator

$$\mathcal{E}_K^2 = \frac{h_K^2}{d_K^3} \|\mathcal{A}(p_h) + \lambda_h + f\|_{0,K}^2 + \frac{1}{2} \frac{h_E}{d_E^3} \|d^3 \llbracket \nabla p_h \cdot \mathbf{n} \rrbracket\|_{0,\partial K}^2 \quad (36)$$

$$+ \|(p_c - p_h)_+\|_K^2 + \int_K (p_h - p_c)_+ \lambda_h \, d\mathbf{x}. \quad (37)$$

Next, we choose an initial mesh \mathcal{C}_h^0 , a value for the parameter $\beta \in (0, 1)$ and a maximum number of iterations k_{\max} , let $k = 1$ and perform the following steps:

- Step 1. Solve the stabilized problem using the mesh \mathcal{C}_h^{k-1} .
- Step 2. Evaluate the error estimator \mathcal{E}_K for each $K \in \mathcal{C}_h^{k-1}$.
- Step 3. Refine the elements that satisfy $\mathcal{E}_K > \beta \max_{K' \in \mathcal{C}_h^{k-1}} \mathcal{E}_{K'}$ and build \mathcal{C}_h^k .
- Step 4. If $k > k_{\max}$ stop, otherwise set $k = k + 1$ and go to Step 1.

An element is refined in Step 3 by adding a vertex at the midpoint of each of its three edges. This larger set of vertices is fed to a mesh generator [35] with an option to include additional points if the shape regularity needs improving.

5. Implementation

The stabilized method of Problem 2 is straightforward to implement using a semismooth Newton's method. This leads to an efficient solution strategy where the reassembly of finite element matrices at each Newton step can be circumvented [20, 27]

Alternatively, the Lagrange multiplier, which is discontinuous across the inter-element boundaries, can be eliminated locally to yield a formulation similar to the traditional penalty method. In fact, letting $\mathcal{H} \in L^2(\Omega)$, $\mathcal{D} \in L^2(\Omega)$ and $\mathcal{A}_h(p_h) \in L^2(\Omega)$ denote the functions satisfying

$$\mathcal{H}|_K = h_K, \quad \mathcal{D}|_K = d_K, \quad \mathcal{A}_h(p_h)|_K = \mathcal{A}(p_h|_K), \quad \forall K \in \mathcal{C}_h, \quad (38)$$

the discrete cavitation region corresponding to p_h becomes

$$\Omega_h^c(p_h) = \{(x, y) \in \Omega : \frac{\mathcal{D}^3}{\alpha \mathcal{H}^2}(p_c - p_h) - f - \mathcal{A}_h(p_h) > 0\}. \quad (39)$$

Defining the discrete forms

$$\begin{aligned} a_h(p_h, q_h; r_h) &= \int_{\Omega_h^c(r_h)} (p_h \mathcal{A}_h(q_h) + \mathcal{A}_h(p_h) q_h + \frac{\mathcal{D}^3}{\alpha \mathcal{H}^2} p_h q_h) \, d\mathbf{x} \\ &\quad - \alpha \int_{\Omega \setminus \Omega_h^c(r_h)} \mathcal{H}^2 \mathcal{A}_h(p_h) \mathcal{A}_h(q_h) \, d\mathbf{x}, \\ L_h(q_h; r_h) &= \int_{\Omega_h^c(r_h)} (p_c \mathcal{A}_h(q_h) + \frac{\mathcal{D}^3}{\alpha \mathcal{H}^2} p_c q_h - f q_h) \, d\mathbf{x} \\ &\quad + \alpha \int_{\Omega \setminus \Omega_h^c(r_h)} \mathcal{H}^2 f \mathcal{A}_h(q_h) \, d\mathbf{x}, \end{aligned}$$

we then arrive at the following formulation of Problem 2.

Problem 3 (Nitsche's method). *Find $p_h \in Q_h$ and the region $\Omega_h^c = \Omega_h^c(p_h)$ such that*

$$\int_{\Omega} d^3 \nabla p_h \cdot \nabla q_h \, d\mathbf{x} + a_h(p_h, q_h; p_h) = \int_{\Omega} f q_h \, d\mathbf{x} + L_h(q_h; p_h), \quad (40)$$

for every $q_h \in Q_h$.

Remark 4. The iterative method for solving Problem 3 reads as: given $p_h^{k-1} \in Q_h$, find $p_h^k \in Q_h, k = 1, 2, \dots$ such that

$$\int_{\Omega} d^3 \nabla p_h^k \cdot \nabla q_h \, d\mathbf{x} + a_h(p_h^k, q_h; p_h^{k-1}) = \int_{\Omega} f q_h \, d\mathbf{x} + L_h(q_h; p_h^{k-1}), \quad (41)$$

for every $q_h \in Q_h$. One starts with an initial guess p_h^0 which solves the unconstrained Reynolds equation and the iteration is terminated when $\|p_h^k - p_h^{k-1}\|$ is small enough. The a posteriori error estimator defined in (37) applies with $\lambda_h = (\frac{\mathcal{D}^3}{\alpha \mathcal{H}^2}(p_c - p_h) - f - \mathcal{A}_h(p_h))_+$.

Remark 5. A similar method was recently proposed by Burman et al. in [36] where the authors recast the classical obstacle problem as an equality for the primal variable. Their method is based on an augmented Lagrangian approach through an elimination of the Lagrange multiplier in the spirit of Chouly and Hild [37]. The extra terms can be interpreted as nonlinear consistent penalty terms.

6. Numerical results

The work of Raimondi–Boyd [38] contains a well-documented and classical application of the Reynolds cavitation model. The authors solve a finite-width journal bearing problem for various configurations using the finite difference method, essentially extending the solution technique of Christopherson [39] to two-dimensional problems. We will consider the same boundary-value problem to highlight the differences between the classical and the proposed numerical procedures. We solve the problem also by the finite element penalty method for which a posteriori error estimators are available and which has often been considered for approximating cavitation problems.

We consider a rectangular domain $\Omega = [0, \frac{2\pi}{3}] \times [0, 1]$. The boundary conditions are $p = 0$ on the whole boundary $\partial\Omega$ and the cavitation pressure is $p_c = 0$. The geometry of the bearing with length-to-radius ratio $L/R = 2$ gives the following operator and loading:

$$\mathcal{A}(p) = \frac{\partial}{\partial\theta} \left(d^3 \frac{\partial p}{\partial\theta} \right) - \frac{1}{4} \frac{\partial}{\partial y} \left(d^3 \frac{\partial p}{\partial y} \right), \quad f = -6 \frac{\partial d}{\partial\theta}, \quad (42)$$

where $d(\theta) = 1 + \varepsilon \cos(\theta - \varphi)$, $\varepsilon = 0.9$ and $\varphi = 0.548388$. Note that due to the chosen eccentricity, the values of the field d^3 vary approximately three orders of magnitude inside the domain.

We solve the described problem using the Nitsche's and penalty methods with linear and quadratic elements. Solutions using higher order elements can be computed by our implementation but their use is counterproductive since the solution has limited regularity. Recall that the penalty method for this problem is essentially the method of Problem 3 with the definitions

$$\begin{aligned} \Omega_h^c(r_h) &= \{(x, y) \in \Omega : p_h < 0\}, \\ a_h(p_h, q_h; r_h) &= \int_{\Omega_h^c(r_h)} \frac{1}{\varepsilon \mathcal{H}^{k+1}} p_h q_h \, d\mathbf{x}, \\ L_h(q_h; r_h) &= 0, \end{aligned}$$

where k is the polynomial degree of the finite element basis and $\varepsilon > 0$ is the penalty parameter. The error estimator for the penalty method is

$$\mathcal{E}_K^2 = \frac{h_K^2}{d_K^3} \|\mathcal{A}(p_h) + \frac{1}{\varepsilon \mathcal{H}^{k+1}} (-p_h)_+ + f\|_{0,K}^2 + \frac{1}{2} \frac{h_E}{d_E^3} \|d^3 \llbracket \nabla p_h \cdot \mathbf{n} \rrbracket\|_{0,\partial K}^2. \quad (43)$$

In each case the mesh is repeatedly refined as described in Section 4. The refinement parameter is chosen as $\beta = 0.5$. The stabilization parameter for the

Nitsche’s method is taken to be $\alpha = 10^{-2}$ which is suitably small for both polynomial degrees. The penalty parameter is chosen quite large, $\epsilon = 10$, since smaller values seem to cause problems for the convergence of the iteration process described in Remark 4—possibly due to the increasing condition number of the system matrix. The iteration counts with respect to the stabilization/penalty parameter are comparable between the two methods. In the penalty method, the number of iterations can be reduced by increasing the value of the penalty parameter which, on the other hand, decreases the accuracy. Nitsche’s method converges fastest if the stabilization parameter is chosen to be close to its upper bound C_I .

The discrete solution, computed with a fine mesh, is visualized in Figure 2. The pressure isolines depicted in Raimondi–Boyd [38] are very similar in shape to ours, and their maximum pressure value 32.8 is close to the one obtained by our implementation, $\max_{\mathbf{x} \in \Omega} p_h(\mathbf{x}) \approx 32.750$. This suggests that the operator and the loading given in (42) have been interpreted correctly for the problem at hand.

Starting with the initial mesh given in Figure 3 (a), we solve, mark and refine four times using the four different methods. The resulting meshes are shown in Figure 3 (b–e). Observe that, with linear elements, the meshes of the stabilized and penalty methods are very similar except for some refinement in the penalty solution in the upper and lower right-hand corners of the cavitated region where, at least intuitively, one would not expect a constant solution needing additional triangles. The problem of unnecessary refinement is more visible when using quadratic elements. The Nitsche’s method leads to a satisfactory mesh with an emphasis on the cavitation boundary where the solution is less regular. The penalty method refines primarily and incorrectly in the area where the solution is known to be constant.

To demonstrate this effect in a more quantitative manner, we start with a coarser mesh and plot the square root of the sum of the error estimators as a function of the number of degrees of freedom, see Figure 4. Note that the sum of the estimators is known to be an upper bound for the true error as indicated by the a posteriori estimates. Again with linear elements both methods perform quite similarly whereas in the quadratic case the Nitsche’s method has a clear edge. The explanation lies in the non-consistency of the penalty approach where the consistency error ultimately limits the rate of convergence, cf. [27].

7. Conclusions

A stabilized method was presented for the adaptive finite element solution of an inequality-constrained Reynolds equation, modeling cavitation in hydrodynamic lubrication, as an alternative to the classical penalty approach. Optimal a priori estimates and new a posteriori error estimators, suitably modified for the governing variable-coefficient obstacle problem, were discussed and the latter were used in numerical experiments.

The positivity constraint on the pressure field was imposed using a Lagrange multiplier which, for being discontinuous, can be eliminated elementwise at the

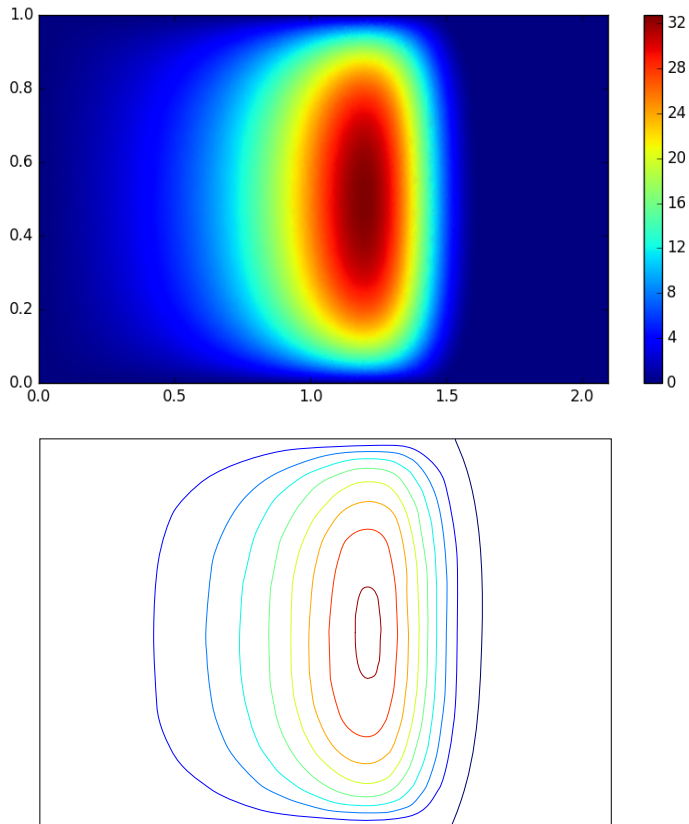
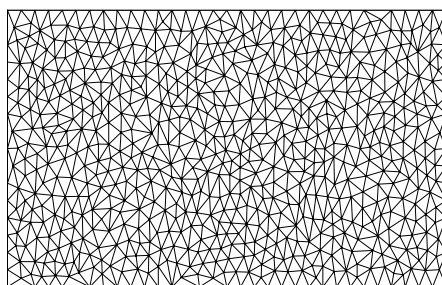


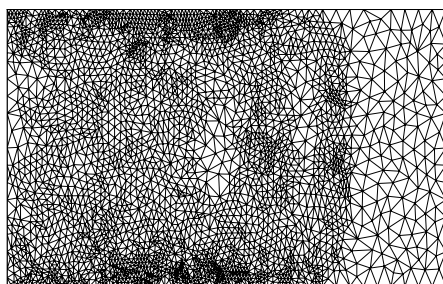
Figure 2: The discrete solution after seven refinements using Nitsche’s method and linear elements is given in the upper panel. The lower panel depicts the pressure isolines at values $0, 4, 8, \dots, 32$ as given in Raimondi–Boyd [38] where the authors report a maximum pressure value of 32.8. Our adaptive method gives the maximum value of 32.750.

discrete level. Hence, the stabilized method could be implemented as a Nitsche-type method which, contrary to the penalty approach, leads to an optimally conditioned, symmetric and positive-definite stiffness matrix. The Nitsche’s method was shown to avoid over-refinement and be well suited for resolving the free boundary related to the initially unknown cavitation region and thus win over the classical penalty method, especially if a quadratic basis is employed.

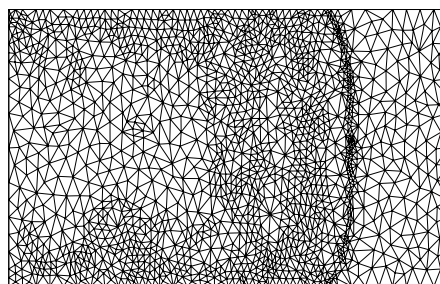
Acknowledgements. Funding from Tekes – the Finnish Funding Agency for Innovation (Decision number 3305/31/2015) and the Finnish Cultural Foundation is gratefully acknowledged, as well as the financial support from FCT/Portugal through UID/MAT/04459/2013 and from the UT Austin-Portugal CoLab Program.



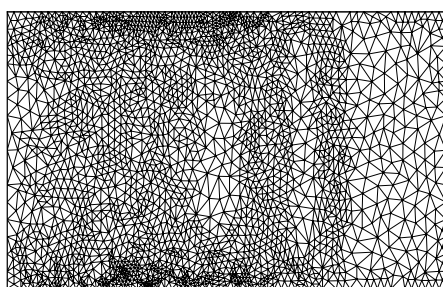
(a) Initial mesh



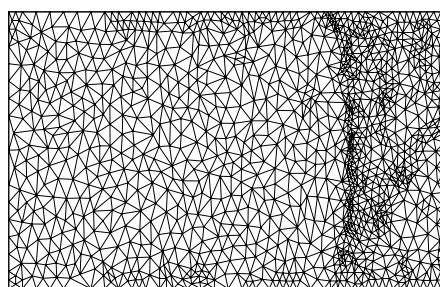
(b) Nitsche, linear elements



(c) Nitsche, quadratic elements



(d) Penalty, linear elements



(e) Penalty, quadratic elements

Figure 3: Initial and final meshes of the different methods after four mesh refinements.

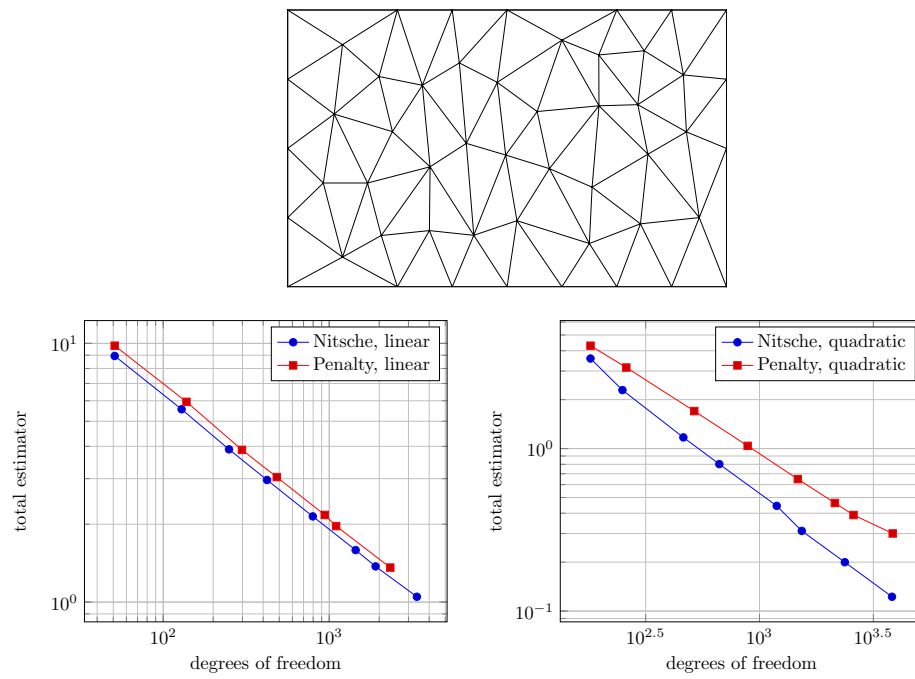


Figure 4: The initial mesh (upper panel) and the resulting global error estimators for the two methods (lower panels), using linear and quadratic elements. The global estimator is defined as the square root of the sum of the elementwise estimators.

References

- [1] O. Reynolds, On the theory of lubrication and its application to Mr. Beauchamp Tower's experiments, including an experimental determination of the viscosity of olive oil., *Proceedings of the Royal Society of London* 40 (242-245) (1886) 191–203.
- [2] K.R. Rajagopal, A. Szeri, On an inconsistency in the derivation of the equations of elastohydrodynamic lubrication, *Proceedings of the Royal Society of London. Series A. Mathematical Physical and Engineering Sciences* 459 (2003) 2771–2786.
- [3] M. Braun, W. Hannon, Cavitation formation and modelling for fluid film bearings: a review, *Proceedings of the Institution of Mechanical Engineers, Part J: Journal of Engineering Tribology* 224 (9) (2010) 839–863.
- [4] C. Xing, M. J. Braun, H. Li, A three-dimensional Navier-Stokes-based numerical model for squeeze-film dampers. Part 1: Effects of gaseous cavitation on pressure distribution and damping coefficients without consideration of inertia, *Tribology Transactions* 52 (5) (2009) 680–694.
- [5] L. Gumbel, Das problem der Lagerreibung, *Monatsblätter Berliner Bezirksvereines deutscher Ingenieure* 5 (1914) 97–104 and 109–120.
- [6] H. W. Swift, The stability of lubricating films in journal bearings, in: *Minutes of the Proceedings of the Institution of Civil Engineers*, Vol. 233, Thomas Telford-ICE Virtual Library, 1932, pp. 267–288.
- [7] W. Stieber, *Des Schwimmlager: hydrodinamische Theorie des Gleitlagers*, VDI-Verlag, GmbH., 1933.
- [8] J.-F. Rodrigues, *Obstacle Problems in Mathematical Physics*, Vol. 134, Elsevier, 1987.
- [9] G. Bayada, C. Vázquez, A survey on mathematical aspects of lubrication problems, *Boletín de la Sociedad Española de Matemática Aplicada* 39 (2007) 31–74.
- [10] H. Elrod, M. Adams, A computer program for cavitation and starvation problems, in: D. Dowson, M. Godet, C. Taylor (Eds.), *Cavitation and Related Phenomena in Lubrication*, Mechanical Engineering Publications, 1974, pp. 37–41, *Proceedings of the 1st Leeds-Lyon Symposium on Tribology*.
- [11] D. Vijayaraghavan, T. Keith Jr, Development and evaluation of a cavitation algorithm, *Tribology Transactions* 32 (2) (1989) 225–233.
- [12] G. Bayada, M. Chabat, M. El Alaoui, Variational formulations and finite element algorithms for cavitation problems, *Journal of Tribology* 112 (2) (1990) 398–403.

- [13] G. Bayada, M. Chambat, A finite element algorithm for cavitation in hydrodynamic lubrication, *Revue Européenne des Eléments* 10 (6-7) (2001) 653–678.
- [14] G. Bayada, V. Carlos, et al., An average flow model of the Reynolds roughness including a mass-flow preserving cavitation model, *Journal of Tribology* 127 (4) (2005) 793–802.
- [15] G. Bayada, M. Chambat, Analysis of a free boundary problem in partial lubrication, *Quarterly of Applied Mathematics* 40 (4) (1983) 369–375.
- [16] A. Almqvist, J. Fabricius, R. Larsson, P. Wall, A new approach for studying cavitation in lubrication, *Journal of Tribology* 136 (1) (2014) 011706.
- [17] G. Garcia, C. Moreno, C. Vazquez, Elrod–Adams cavitation model for a new nonlinear Reynolds equation in piezoviscous hydrodynamic lubrication, *Applied Mathematical Modelling* 44 (0) (2017) 374–389.
- [18] K. Mistry, S. Biswas, K. Athre, A new theoretical model for analysis of the fluid film in the cavitation zone of a journal bearing, *Journal of Tribology* 119 (1997) 741.
- [19] M. Lanzendörfer, J. Málek, K. R. Rajagopal, Numerical simulations of an incompressible piezoviscous fluid flowing in a plane slider bearing, *Meccanica* 53 (1-2) (2018) 209–228.
- [20] T. Gustafsson, R. Stenberg, J. Videman, Mixed and stabilized finite element methods for the obstacle problem, *SIAM Journal on Numerical Analysis* 55 (6) (2017) 2718–2744.
- [21] M. Juntunen, R. Stenberg, Nitsche’s method for general boundary conditions, *Mathematics of Computation* 78 (267) (2009) 1353–1374.
- [22] A. Sorsimo, M. Juntunen, R. Stenberg, J. Videman, Finite element analysis of the Reynolds lubrication equation with cavitation, *Journal of Structural Mechanics* 45 (4) (2012) 188–200.
- [23] T. J. Hughes, L. P. Franca, A new finite element formulation for computational fluid dynamics: VII. the Stokes problem with various well-posed boundary conditions: symmetric formulations that converge for all velocity/pressure spaces, *Computer Methods in Applied Mechanics and Engineering* 65 (1) (1987) 85–96.
- [24] S. Wu, J. Oden, A note on applications of adaptive finite elements to elasto-hydrodynamic lubrication problems, *Communications in Applied Numerical Methods* 3 (6) (1987) 485–494.
- [25] B. Nilsson, P. Hansbo, Adaptive finite element methods for hydrodynamic lubrication with cavitation, *International Journal for Numerical Methods in Engineering* 72 (13) (2007) 1584–1604.

- [26] C. Johnson, Adaptive finite element methods for the obstacle problem, *Mathematical Models and Methods in Applied Sciences* 2 (04) (1992) 483–487.
- [27] T. Gustafsson, R. Stenberg, J. Videman, On finite element formulations for the obstacle problem – mixed and stabilised methods, *Computational Methods in Applied Mathematics* 17 (3) (2017) 413–429.
- [28] C. Bernardi, R. Verfürth, Adaptive finite element methods for elliptic equations with non-smooth coefficients, *Numerische Mathematik* 85 (2000) 579–608.
- [29] W. Dörfler, O. Wilderotter, An adaptive finite element method for a linear elliptic equation with variable coefficients, *ZAMM* 80 (7) (2000) 481–491.
- [30] A. Z. Szeri, *Fluid Film Lubrication: Theory and Design*, Cambridge University Press, 2005.
- [31] B. J. Hamrock, S. R. Schmid, B. O. Jacobson, *Fundamentals of Fluid Film Lubrication*, CRC Press, 2004.
- [32] T. Gustafsson, K. Rajagopal, R. Stenberg, J. Videman, Nonlinear Reynolds equation for hydrodynamic lubrication, *Applied Mathematical Modelling* 39 (17) (2015) 5299–5309.
- [33] S. Nazarov, J. Videman, A modified nonlinear Reynolds equation for thin viscous flows in lubrication, *Asymptotic Analysis* 52 (2007) 1–36.
- [34] R. Verfürth, *A Posteriori Error Estimation Techniques for Finite Element Methods*, Oxford University Press, 2013.
- [35] J. R. Shewchuk, Triangle: Engineering a 2D quality mesh generator and Delaunay triangulator, in: M. C. Lin, D. Manocha (Eds.), *Applied Computational Geometry towards Geometric Engineering*, Vol. 1148 of *Lecture Notes in Computer Science*, Springer, 1996, pp. 203–222.
- [36] E. Burman, P. Hansbo, M. G. Larson, R. Stenberg, Galerkin least squares finite element method for the obstacle problem, *Computer Methods in Applied Mechanics and Engineering* 313 (2017) 362–374.
- [37] F. Chouly, P. Hild, Nitsche-based method for unilateral contact problems: numerical analysis, *SIAM Journal on Numerical Analysis* 51 (2) (2013) 1295–1307.
- [38] A. Raimondi, J. Boyd, A solution for the finite journal bearing and its application to analysis and design: III, *ASLE Transactions* 1 (1) (1958) 194–209.
- [39] D. G. Christopherson, A new mathematical method for the solution of film lubrication problems, *Proceedings of the Institution of Mechanical Engineers* 146 (1) (1941) 126–135.